Preliminary Observations of Resonance Enhanced Raman Scattering in Liquid Benzene

Todd Chadwick[†], Dr. Hans Hallen[†]   &   Adam Willitsford[‡], Dr. C. Russell Philbrick[‡]

[†]Department of Physics, North Carolina State University   [‡]Department of Electrical Engineering, Pennsylvania State University

1. Introduction

1.1 Conventional Raman Scattering

Raman scattering has been intensely investigated since its discovery in 1928 by C.V. Raman. This discovery was so profound and useful to the advancement of science Raman was awarded the Nobel Prize for his efforts in optical scattering in 1930. Raman scattering is a process by which light scatters from a molecule at a different wavelength or energy than that which excited the molecule. The difference in wavelength can be accounted for by the vibrational or rotational transitions of the molecule. Because the vibrational and rotational levels are unique to each molecule, Raman spectroscopy is a powerful tool for locating, identifying and quantifying unknown chemical or biological agents. Figure 1 exhibits a typical Raman line for diamond.

Figure 1: $1331.5\,cm^{-1}$ *Stokes Line for Diamond*

There are 2 types of Raman scattering: Stokes results when the scattered radiation is at a lower energy or longer wavelength than the incident radiation and anti-Stokes results when the scattered radiation is at a higher energy or shorter wavelength than the incident radiation. Because more molecules are in their rest state than in an excited state, Stokes Raman scattering is more probable. Table 1 shows the difference in scattering cross-sections for various optical interactions.

**Table 1:** *Optical Scattering Cross-sections* $(\frac{d\sigma}{d\Omega})$

Interaction	Process	Frequency Relation	Cross-Section $(\frac{cm^2}{sr})$	Detectable Constituents
Scattering	Mie	$\nu_r = \nu_0$	$10^{-26} - 10^{-8}$	Particulate Matter
	Rayleigh	$\nu_r = \nu_0$	10^{-26} (NR) 10^{-23} (R)	Atoms & Molecules
	Raman	$\nu_r \neq \nu_0$	10^{-29} (NR) 10^{-26} (R)	Molecules (atoms)
Emission	Fluorescence	$\nu_r = \nu_0$	10^{-26} (Quenched) 10^{-24} (Quenched)	Atoms & Molecules
Absorption		$\nu_r = \nu_0$	10^{-20}	Atoms & Molecules

ν_r: Detection Frequency, ν_0: Laser Frequency; NR: Non-Resonance, R: Resonance, (Inaba)

1.2 Resonance Raman Scattering

Resonance Raman scattering occurs when the incident wavelength falls within an electronic absorption band of the molecule, causing the vibrations of the absorbing specie to be enhanced. This scattering enhancement can be as much as 6 orders of magnitude larger than classical Raman scattering. Although the resonance effect greatly enhances the scattering power this effect is not always easily observed, the simultaneously intensified absorption and the concealing effects of fluorescence may hide the Raman scattered radiation. Figure 2 shows a comparison of Raman scattering, preresonance Raman, resonance Raman and fluorescence.

Figure 2: *Optical Scattering Processes*
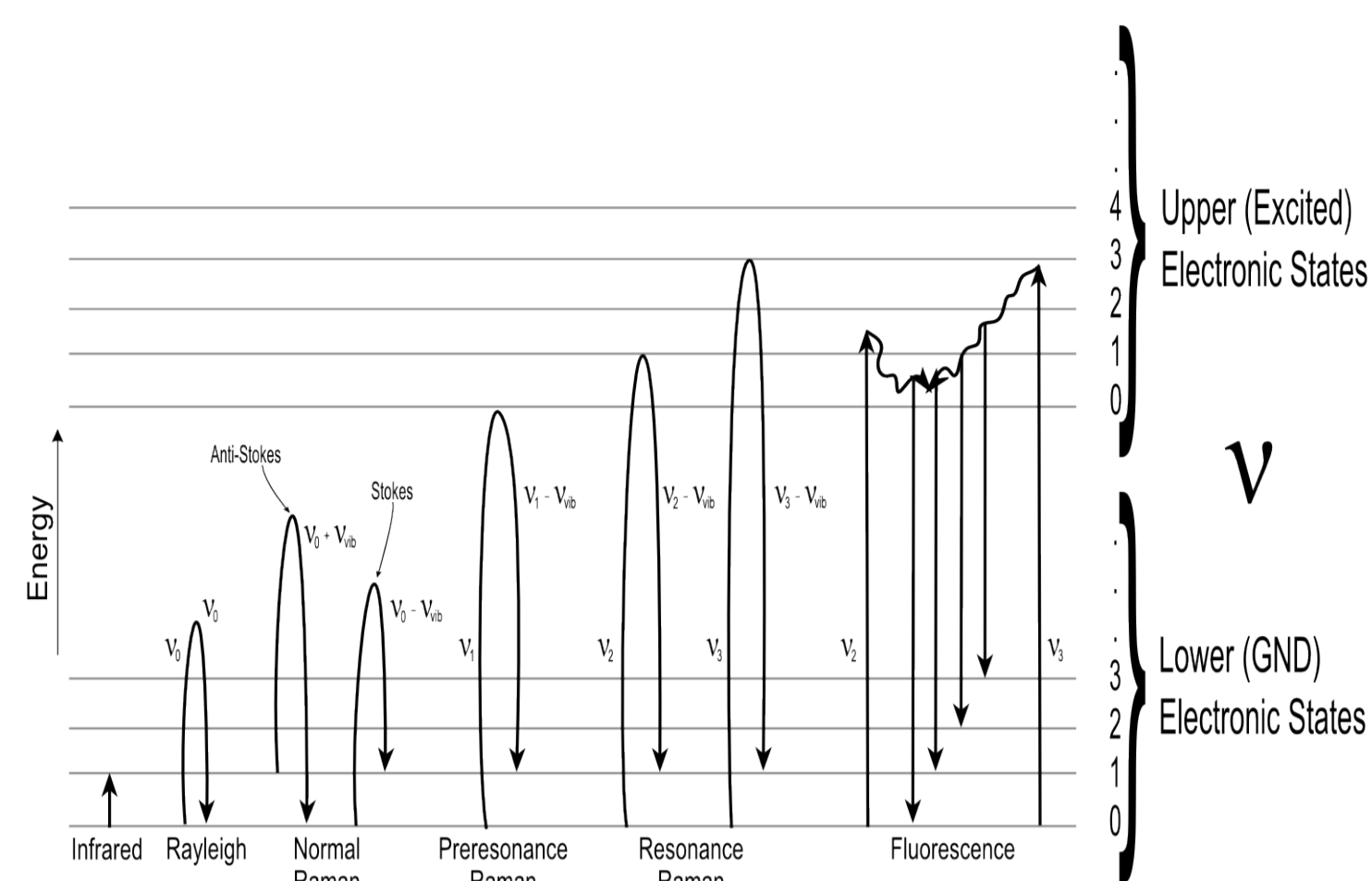
When working in the resonant Raman enhancement region, the fluorescent effects may also be enhanced. Although the fluorescent signal is quite large it is also very broad and *vague* in its identification. Fluorescence occurs with limited specificity to the scattering medium. So it may be *possible* to use fluorescence as a detection means, but not for identification. Currently, no known material fluoresces with any significant intensity below $\approx 280\,nm$. With the Raman scattering spectral range of $4160\,cm^{-1}$, this allows for complete separation of the fluorescent emissions from the Raman emission for incident $\lambda \leq 250\,nm$.

Resonance Raman scattering can provide significantly enhanced Raman emissions $10^3 - 10^8$ times larger than normal Raman scattering. Nearly every material maintains a unique Raman spectra, however in the case of pollutants, explosives or biological contaminants the number density is generally quite small ($\approx \frac{10^{17}}{cm^3}$). These examples are perfect cases where the use of resonance enhanced Raman scattering can be employed to detect ultra-small quantities that are $10^3 - 10^8$ times less concentrated than usual atmospheric contents.

2. The Experiment

We expect to find resonance Raman enhancement in the electronic transitions which correspond to peaks in the absorption spectra. Based on preliminary searches of absorption spectra, we selected materials with steep absorption profiles at wavelengths we could scan with our tunable UV source. Benzene was particularly interesting with its sharp peaks and structure (see Figure 3). Tuning through either side of a steep absorption structure should show a spike in the observed Raman signal at the maximum absorption. Akin to vibrational resonance we have intensity of vibrations I such that:

$$I(\omega) \propto \frac{1}{\omega^2 - \omega_0^2 - r\gamma}.$$

Having sharp peaks makes tuning about the maximum absorption quickly observable.

**Figure 3:** *Absorption Spectra for liquid benzene*
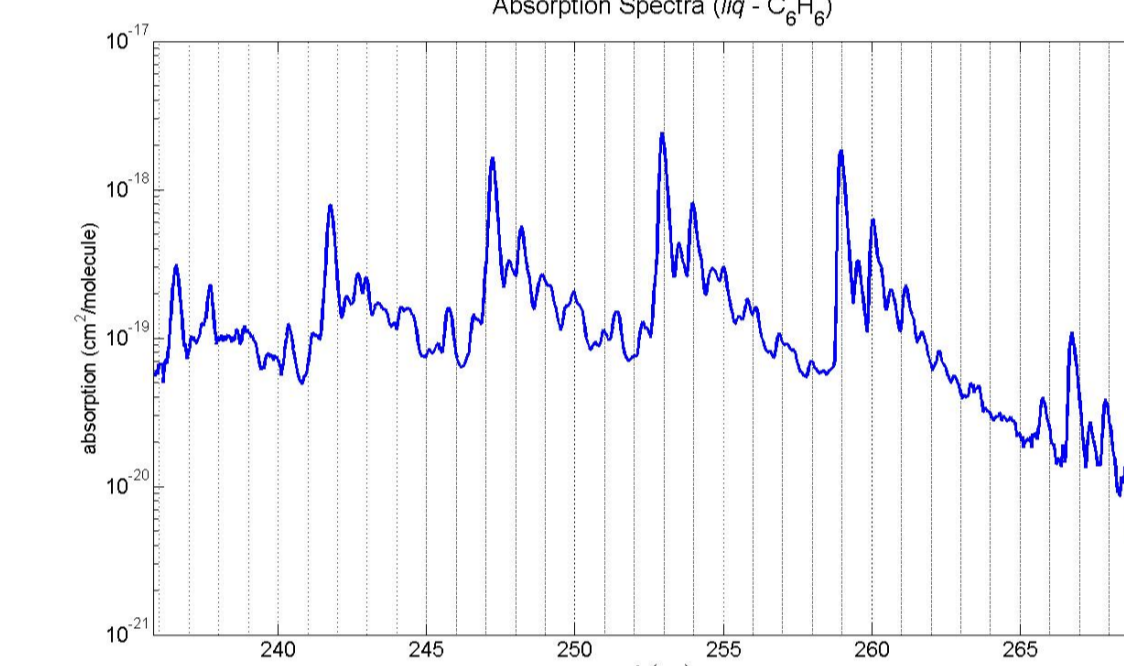
3. Resonance Raman Results

3.1 Observations

As expected (*in retrospect*), a clear enhancement is observed in benzene (Figure 4). The sharp peak has a 2-fold effect: 1st because of the narrow band, the dampening of the resonant effect is negligible, 2nd the Raman scattered light is then off of the absorption peak allowing for detection.

Figure 4: $2\,nm$ *Scan About* $259\,nm$ *On Liquid Benzene*
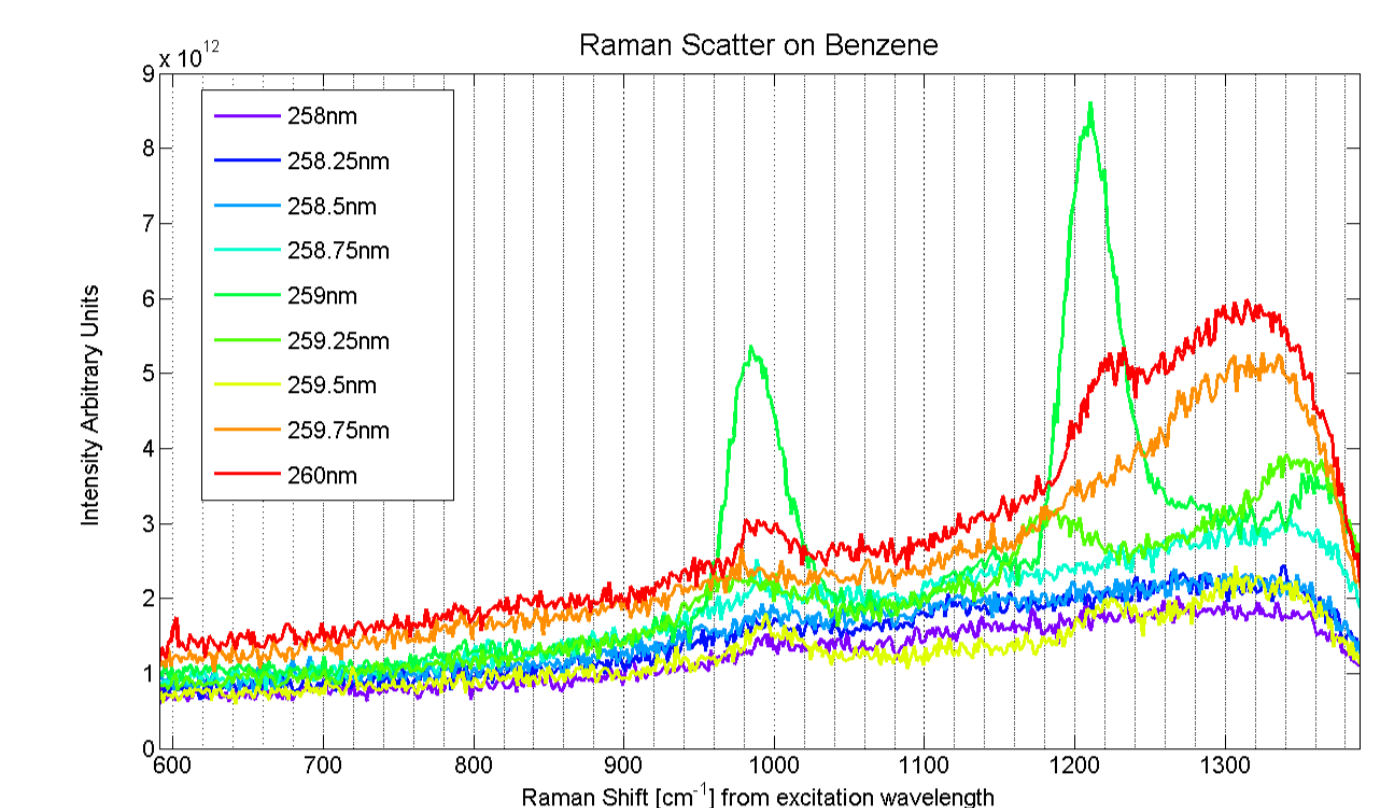

When off resonance the ν_2 line at $\approx 995\,cm^{-1}$ is the strongest, however when at (*near*) resonance, a large relative increase in the $1210\,cm^{-1}$ signal is observed ($\sim 2X$ as strong as the signal observed at $995\,cm^{-1}$). **When the Raman lines are compared to their visible Raman scatter counterparts at $450\,nm$ the differential Raman scattering cross section of benzene is approximately 5000 times larger when on resonance at $259\,nm$.**

3.2 Lamentations On The Observations

Initially we thought this resonance was attributable to a shifted $1178\,cm^{-1}\,\nu_{17}$ line. However, further contemplation suggests the line is the result of a multi-photon process at the $605\,cm^{-1}\,\nu_{18}$, leading to our observed $1210\,cm^{-1}\,2\nu_{18}$ signal. Looking at the $605\,cm^{-1}$ line for $259\,nm$ we have no signal, which *is* observable at our off-resonance excitation reference at $450\,nm$.

4. Tunable UV: Optical Parametric Oscillator

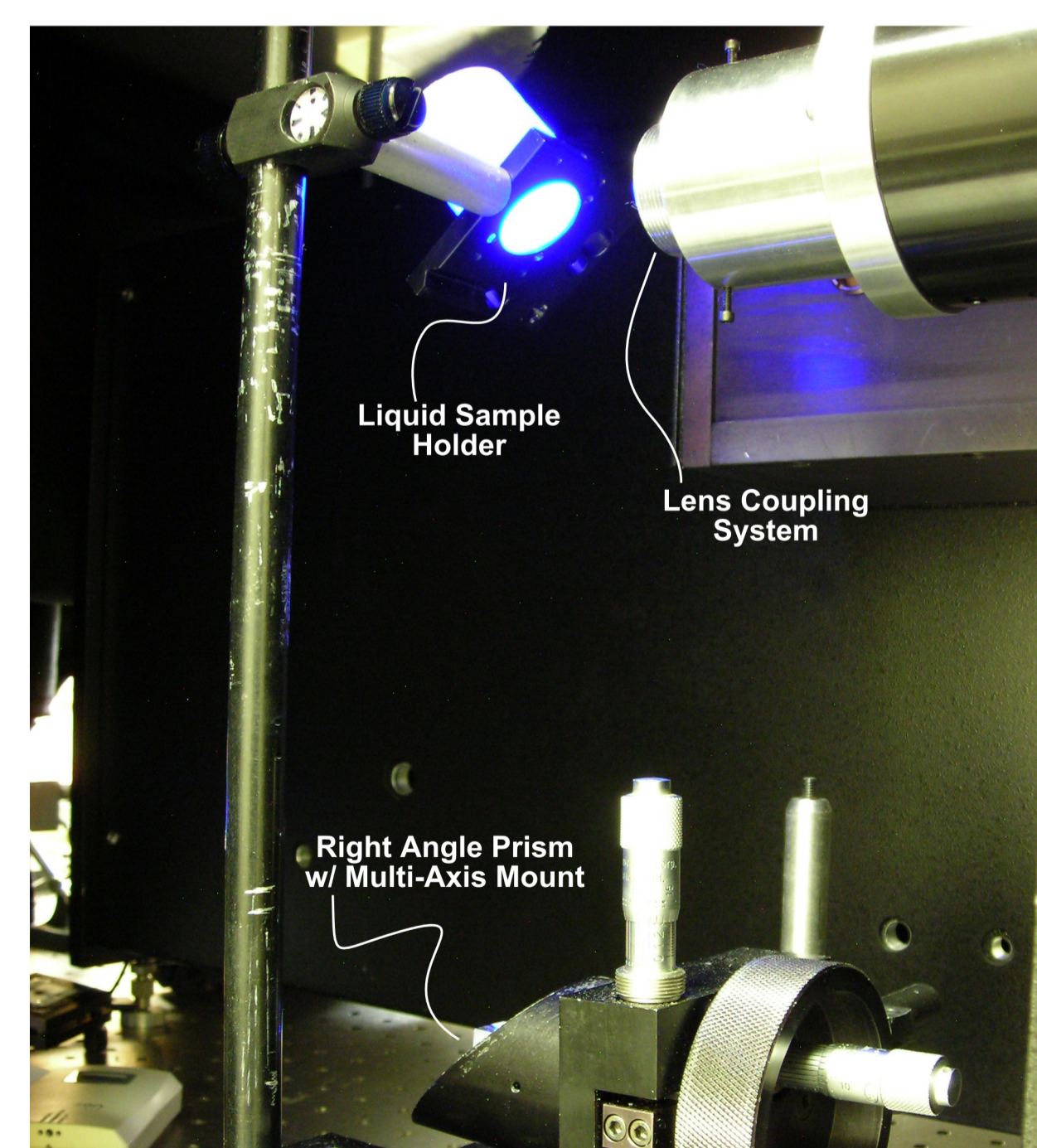**Figure 5:** *OPO Cavity Detail*
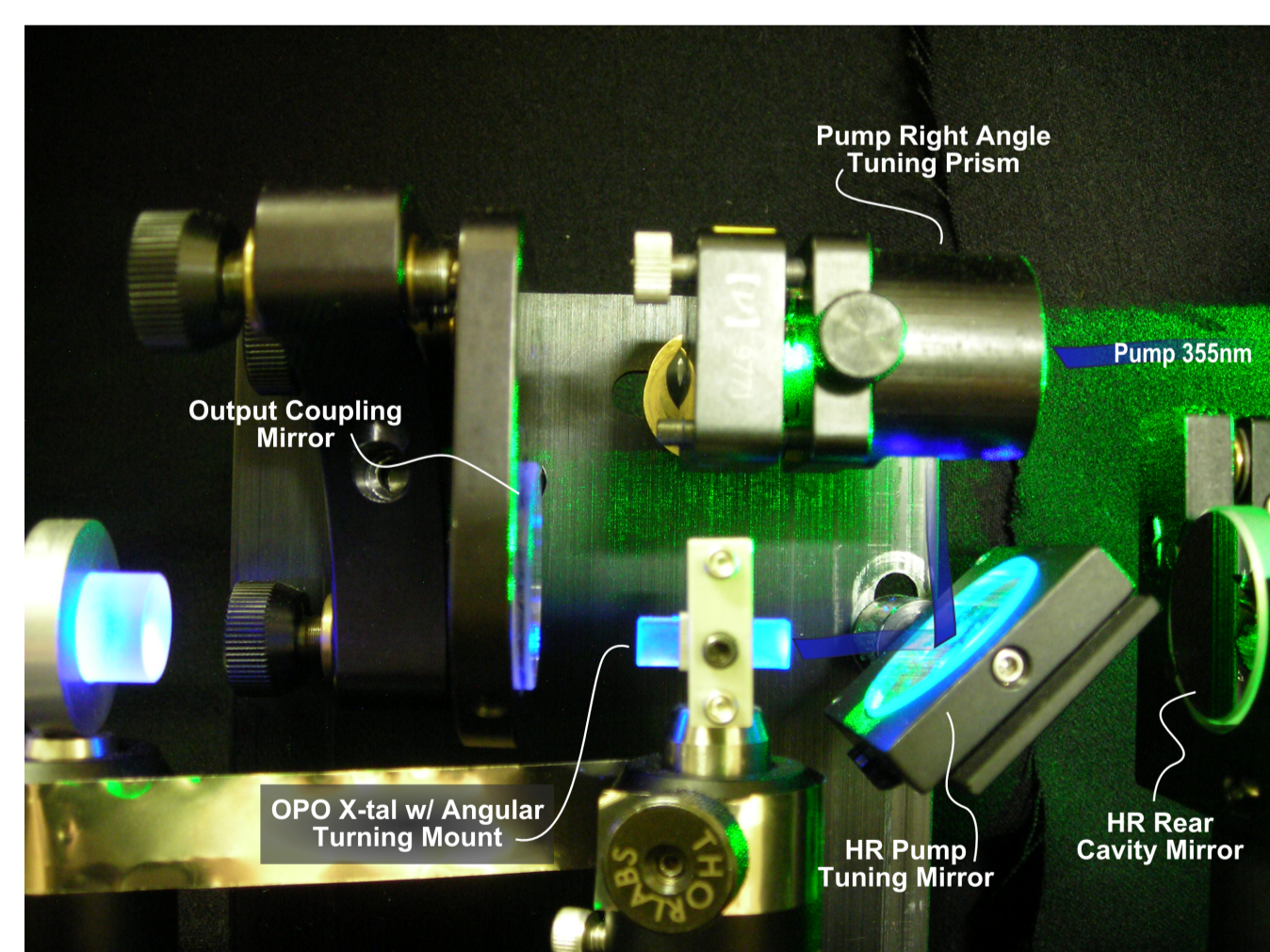
An optical parametric oscillator (OPO) is a tunable optical cavity that is capable of generating continuous (in λ) laser spectra. An OPO contains the basic makeup of a laser: cavity mirrors, a pump source, and an excitable optical medium. The pump source in the case of our OPO is the 3ω harmonic of the Nd:YAG laser at $354.7\,nm$. This beam is then split within the OPO cavity into 2 other beams a signal and an idler. Figure 5 details our OPO cavity. As with usual nonlinear optical processes, the frequencies in our OPO obey: $\omega_{pump} = \omega_{signal} + \omega_{idler}$.

Our useful output (ω_{signal}) is in the visible. We make use of a $\beta - BBO$ (Beta-Barium Borate) crystal which is well suited for nonlinear generation because of its high nonlinear optical coefficient as well as its high damage threshold ($> \frac{1\,GW}{cm^2}$). Tuning (phase matching) is accomplished by angular positioning of the $\beta - BBO$ crystal relative to the pump. The phase matching conditions for our OPO cavity are shown in Table 2. To achieve a tunable UV output we simply double ω_{signal} via similar $\beta - BBO$ crystals cut for 2ω harmonics. With this we have an entire tuning range from $210\,nm - 2200\,nm$ out of the OPO.

5. Spectrometer Configuration

Figure 6: $90°$ *Scattering Configuration*

A $90°$ optical scattering setup was utilized for collection of the Raman spectra. The incident light illuminates the sample at $\approx 45°$. Raman scattering is isotropic so collection of the emissions is via a matched lens system to collimate and focus the scattered light into the spectrometer's entrance slit. The light travels through the spectrometer, separates via a ruled diffraction grating, with the different wavelengths becoming spatially separated making it possible to image different wavelengths along a CCD camera.

For our Raman observations, this optical path becomes significant: *small spectrometers lack the resolving capabilities for closely spaced Raman wavelengths*. An initial run with a $0.3\,m$ single stage spectrometer provided observation of this limitation. Switching to a triple stage $0.6\,m$ version we are able to achieve overall stray-light rejection on the order of 10^{-14}. This has provided improved resolution ($4X$) and enhanced our S/N ratio over our previous attempts. Figure 6 details our current setup.

References

[1] P.R. Carey *Biochemical Applications of Raman and Resonance Raman Spectroscopies*, (1982) Academic Press New York

[2] T. Etzkorn, B.Klotz, S. Sørensen, I.V. Patroescu, I. Barnes, K.H. Becker, U. Platt "Gas-Phase absorption cross sections of 24 monocyclic aromatic hydrocarbons in the UV and IR spectral ranges", *Atmos. Environ.*, **33** 525 (1999)

[3] G. Herzberg *Molecular Spectra and Molecular Structure*, (1945) D. Van Nostrand Company Princeton

[4] H. Inaba "Detection of Atoms and Molecules by Raman Scattering and Resonance Fluorescence", *Laser Monitoring of the Atmosphere* (1976) Springer-Verlag New York

[5] Knight D.S. and W.B. White "Characterization of diamond films by Raman spectroscopy", *J. Mater. Res.*, **4, No.2** 385 (1989)

[6] A.J. Melveger *Resonance Raman spectroscopy as an analytical tool*, (1978) The Franklin Institute Press Philadelphia

[7] Raman C.V. "A Change of Wavelength in Light Scattering", *Nature* (1928)

[8] Ziegler L.D. and B. Hudson "Resonance Raman scattering of benzene and benzene-d_6 with 212.8 nm excitation", *J. Chem Phys.*, **74, No.2** 982 (1981)